Analysis of Reaction Kinetics of End-Functionalized Polymers at a PS/P2VP Interface by DSIMS

Bumjoon J. Kim,[†] Glenn H. Fredrickson,[†,‡] and Edward J. Kramer*[,†,‡]

Department of Chemical Engineering and Department of Materials, University of California, Santa Barbara, California 93106

Received May 18, 2006; Revised Manuscript Received October 28, 2006

ABSTRACT: Reactions to produce graft copolymers at polymer interfaces during extruder mixing are important for controlling dispersed phase size by retarding droplet coalescence and reducing interfacial tension while reinforcing the polymer interface. Such reactions are investigated at various temperatures in a model bilayer film system consisting of amine end-functional deuterated polystyrene (dPS-NH_2) in PS and anhydride end-functional poly(2-vinylpyridine) (P2VP-ah) in P2VP. The interfacial excess (z^*) of block copolymer formed by the reaction of dPS-NH_2 and P2VP-ah at the interface is determined by detecting the $^2H^-$ ion using dynamic secondary ion mass spectrometry (DSIMS). The reaction kinetics is analyzed using a model based on a reaction-controlled mechanism for various reaction temperatures and molecular weights (M_n) of the end-functional chains. At low initial volume fractions ϕ_0 ($\sim$0.01) of dPS-NH_2 and P2VP-ah, such that the normalized interface excess (z^*/R_g) < 1 and the blocks are unstretched, the forward reaction rate constant (k^+) decreases as $M_n^{-0.70}$, in rough agreement with predictions of the model ($k^+ \sim M_n^{-0.55}$) for this regime. The reaction is thermally activated with an activation enthalpy ($\sim$160 kJ/mol) that is independent of M_n. The interfacial reaction, which is carried out under high-vacuum conditions so that any water produced by reaction would be efficiently removed, is reversible with an equilibrium constant K_{rxn} that has an enthalpy of reaction of -55 kJ/mol. This result means that the interface reaction does not proceed to form the cyclic imide, but likely stops at the amic acid.

Introduction

Reactive blending using in-situ reactive compatibilizers is one of most efficient ways to develop new polymeric materials with desired properties. Compatibilizers such as diblock and graft copolymers formed by reaction are very effective in strengthening the interface between immiscible polymers and controlling dispersed phases by suppressing coalescence of droplets, even at very low areal chain densities. In particular, forming the compatibilizers at the interface by reaction of the reactive polymers avoids many of the shortcomings of adding premade block and graft copolymers. In most such cases blending of premade copolymers leads to most of them being sequestered in micelles and, as a consequence, their very slow delivery to the interfaces.[1,2] However, establishing the reaction kinetics of these compatibilizers at the interface is crucial for understanding such reactive blending. The reaction kinetics have been investigated theoretically by several other researchers based on either reaction-controlled or diffusion-controlled models.[3−9] Many theoretical treatments[3,4,6,7] of these reaction kinetics are based on the assumption that the reaction kinetics are controlled by diffusion of reactive polymers rather than reaction. Fredrickson and Milner found out that the growth of a copolymer layer by reaction can be characterized by different regimes based on their characteristic time scales. They predicted a crossover from diffusion-limited behavior, accompanied by a depletion hole of the reactive species next to the interface, to saturation behavior due to the dramatic increase in chain stretching penalty of polymer brushes at the interface. However, in many practical cases, the characteristic time scale for reaction may be much longer than that for diffusion at the typical interface separations in polymer blends. Kramer[5] constructed a model of grafting kinetics for two different cases where the formation of copolymer at the interface is controlled by diffusion of reactive polymers and by reaction of polymers at the interface. He found that the growth of copolymer can be expressed as the same form of reaction kinetics, but with different characteristic times. Oyama et al.[9] analyzed the reaction kinetics for reactive polymer blends of amorphous polyamide (amine end groups)/end-functional polysulfone, styrene−maleic anhydride copolymer/amine-terminated butadiene−acrylonitrile copolymer, and carboxyl end-functional polystyrene/precured epoxy containing excess epoxide groups. They showed that a reaction-controlled model with pseudo-first-order reaction kinetics could fit the data since in each case the concentration of one reactive polymer group did not change significantly with time during the reaction. In the more general case, such as the experiments reported below, where both reactive species are expected to be depleted as the reaction progresses, a reaction-controlled model with second-order reaction kinetics must be used, however.

Several research groups have investigated reaction progress in reactive blends experimentally either by observing the decrease in domain size of dispersed phases as reaction proceeds or by measuring the amount of coupling by size exclusion chromatography (SEC).[10−13] However, the reactive blends in those studies are usually prepared in a mixer or extruder, with accompanying complex melt flows leading to a total interfacial area that increases with the time of reaction. The growth rate of the copolymer layer is difficult to determine accurately in such cases due to this change in interfacial area. Furthermore, the interfacial area is also affected by the decrease of interfacial tension that accompanies copolymer formation in many cases, a decrease that can induce the formation of either micelles or microemulsified droplets.[14,15] It should be noted, however, that recent experiments have been reported on multilayer film, either reacted under quiescent conditions or while being subjected to oscillatory shear parallel to the layers.[33,34] In both cases the layer

* Corresponding author. E-mail: edkramer@mrl.ucsb.edu.
[†] Department of Chemical Engineering.
[‡] Department of Materials.

10.1021/ma0611218 CCC: $37.00
Published on Web 04/11/2007

interfaces remained flat so no additional interfacial area was created yet the reaction was much faster under oscillatory shear. The origins of this increased reactivity are currently unknown.

Even though they may not fully represent the reaction under flow conditions, model studies of reaction kinetics under quiescent conditions are useful for understanding of diffusion and reaction of reactive polymers at interfaces. Most such experiments to date are based on samples consisting of bilayers of immiscible polymers with a planar geometry. Some research groups have investigated reaction kinetics based on the system of bilayers consisting of immiscible polystyrene (PS) and poly(methyl methacrylate) (PMMA).[15−18] Yin et al.[18] and Schulze et al.[17] probed the reaction progress by SEC using anthracene-labeled reactive polymers to increase the sensitivity. Schulze et al.[16,17] also investigated the reaction progress using forward recoil spectrometry (FRES) to depth profile deuterium-labeled reactive chains at and near the interface with 90 nm depth resolution. Kim et al.[15] investigated the reaction kinetics using a rheological method and correlated morphological changes at the interface with rheological properties. However, since the bilayer samples in their system were composed of only reactive PS and high wt % of reactive PMMA chains in PMMA (10% to 100%), it was difficult to investigate a wide range of chain areal density at the interface. For example, they could not attain a low enough chain areal density to exclude interfacial roughening.[15,19−21] It is found that once the chain areal density of polymer brushes at the interface exceeds a critical value, the interface becomes rough, inducing the formation of micelles or microemulsified droplets in many cases. In such cases the true interfacial chain areal density cannot be estimated from the amount of coupled reactive polymers measured by SEC. This disadvantage can be overcome by keeping the chain areal density low enough to prevent interfacial roughening by lowering the concentration of reactive groups, i.e., diluting the reactive polymers in each layer with unreactive homopolymer. This procedure simulates the practical situation where only small volume fractions of reactive polymers are added to the homopolymers being blended in order to minimize cost. Many theoretical predictions as well as experimental results show that the chain areal density saturates due to a dramatic increase in the entropy penalty caused by chain stretching as the copolymers are packed into a dense brush at the interface. Therefore, since the model for reaction kinetics in the mushroom regime can be simplified by assuming that the chain stretching penalty is negligible, the comparison of the model with the experimental results becomes more straightforward at these low chain areal densities.

The end-functionalized polymers, deuterated polystyrene (dPS) with a terminal amine end group and poly(2-vinylpyridine) (P2VP) with a terminal anhydride end group, are used as a model reactive system. The use of PS and P2VP is advantageous for several reasons as mentioned in a previous paper.[14] These advantages of PS and P2VP help us investigate diffusion as well as reaction of the end-functionalized polymers in our system. In addition, there is considerable information on the reaction between polymers with anhydride and amine end-functional groups in the literature.[22,23] The reaction of amines with anhydrides has been shown to be fast enough in the melt to be of interest for commercial utilization in reactive blending. All experiments were designed so that the block copolymers formed by end-functionalized polymers with small molecular weight were formed at the interface between an immiscible bilayer of PS and P2VP homopolymers with relatively high molecular weight. Therefore, the diffusion coefficients of end-functionalized polymers in the homopolymer matrix of our system can be estimated on the basis of the work of Green and Kramer.[24] In addition, as mentioned in the previous paragraph, the grafting density regime in the experiment needs to be low enough to minimize any chain stretching penalty and, at the same time, high enough to be determined accurately by experiment, in our case by depth profiling using dynamic secondary ion mass spectrometry (DSIMS).

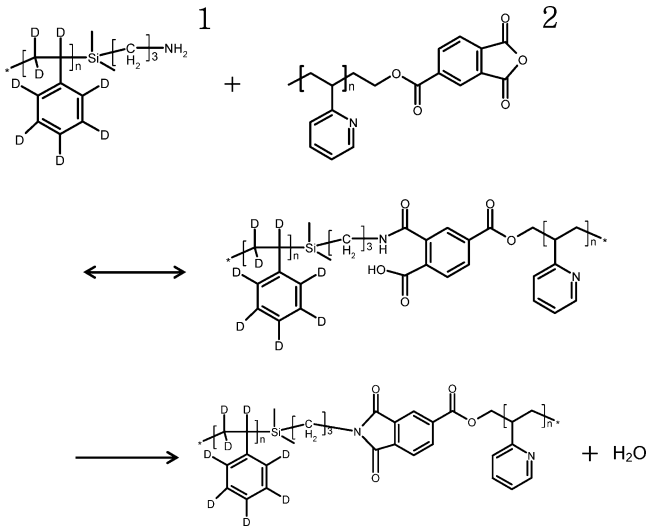

Figure 1. Chemical reaction that takes place at the interface. Deuterated PS with an amine end group reacts with P2VP with an anhydride end group to form dPS-P2VP diblock copolymer.

In this paper, we develop a kinetic model of reaction-controlled grafting based on a second-order reaction rate equation and compare it to our experimental results obtained in the low grafting density regime where the chains in the block copolymer layer at the interface are not stretched, so there is no chain stretching entropy penalty and the interface remains flat. The reaction progress is monitored quantitatively by measuring the normalized interfacial excess using dynamic secondary ion mass spectrometry (DSIMS). DSIMS, a well-established depth-profiling technique, is applied to monitor the reaction and diffusion of the deuterium-labeled amine end-functionalized PS (dPS-NH_2). Recent experiments by Harton et al. show that DSIMS can be very useful for separating the effects of diffusion and reaction at polymer interfaces.[35] DSIMS has much better depth resolution (∼8 nm) than FRES (∼90 nm) combined with high sensitivity and the ability to provide the profiles of all elements at the same time. The growth of chain areal density at the interface is measured for a series of end-functional PS with various molecular weights at different reaction temperatures. The information gives us an estimate for the reaction rate at the interface as a function of the molecular weight of reactive polymers and reaction temperatures. The dependence of the reaction kinetics on the molecular weight of reactive polymers and reaction temperatures can be compared directly to the prediction from the reaction-controlled model described in this paper. In addition, we will discuss the reversibility of the reaction in the system. The combination of these experimental conditions and techniques makes our system close to an ideal model experiment for comparison with the reaction kinetics model.

Experimental Section

Polymer Synthesis and Characterization. An amine end-functionalized deuterated polystyrene (dPS-NH_2), shown as **1** in Figure 1, was synthesized by living anionic polymerization.[25]

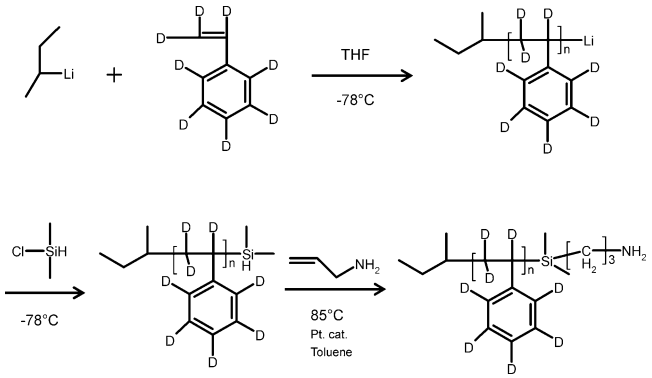

Figure 2. Schematic for synthesis of amine end-functional deuterated PS (dPS-NH_2). dPS anions were terminated by chlorodimethylsilane. A hydrosilylation reaction with allylamine introduces a primary amine group at the end of dPS.

Table 1. Characteristics of Polymers Used in Present Study

polymer	M_n (kg/mol)	M_w/M_n	functionality
PS	207	1.06	
P2VP	152	1.12	
dPS-NH_2	7	1.05	0.89,[a] 0.86[b]
	11	1.10	0.95,[a] 0.60[b]
	17	1.10	0.64[b]
	21	1.05	0.45[b]
	26	1.03	0.43[b]
P2VP-ah	8,[c] 6[d]	1.03	0.3[e]

[a] Measured by titration. [b] Measured by NMR. [c] Measured by MALDI. [d] Measured by SEC. [e] Obtained by coupling with PEG-NH_2 (M_n = 5K) and measuring the ratio of coupled product to unreacted polymers using SEC.

Deuterated styrene monomers were dried over dibutylmagnesium for 3 h. Tetrahydrofuran (THF) was dried using an alumina column and *sec*-butyllithium. Next, THF was distilled into the reaction vessel. Styrene monomers were added to the THF, and the polymerization was initiated by the addition of a calculated amount of *sec*-butyllithium at −78 °C. After completion of the polymerization (3 h), the living anions were terminated with chlorodimethylsilane at −78 °C. Then, THF solvent was removed under vacuum after the temperature was raised to room temperature, and anhydrous toluene was added to dissolve the dPS. Allylamine was added with an equal mole ratio to the silane-terminated dPS, and a few drops of Pt catalyst were then added to the polymer solution; further reaction was carried out at 85 °C overnight. An anhydride end-functionalized poly(2-vinylpyridine) (P2VP-ah), **2** in Figure 1, was prepared by anionic polymerization as described elsewhere.[14] A P2VP homopolymer was also synthesized by anionic polymerization and was terminated by degassed 1-butanol. A PS homopolymer was kindly donated by Dow Chemical.

The characteristics of the polymers used in present study are summarized in Table 1. The molecular weight and polydispersity of dPS-NH_2 were determined by size exclusion chromatography (SEC) using PS standards. The polydispersity of the amine end-functionalized polymers becomes broader than that before attachment of amine group, possibly due to the interaction of the amine group and the SEC column. Therefore, the values of polydispersity in the table are obtained from those before amine functionalization. The functionality of dPS-NH_2 was determined by ^{1}H-NMR by comparing the signals from the aliphatic protons next to the terminal amine group to the proton signals from the *sec*-butyllithium initiator. For the lower molecular weights the NMR results were double checked by titrating the dPS-NH_2 polymer with $HClO_4$ to a violet end point in a 1:1 v/v solution of chloroform and glacial acetic acid using crystal violet as an indicator. In calculations the measured dPS-NH_2 volume fractions far from the interface were corrected using the NMR functionality. The molecular weight and polydispersity of the P2VP-ah were determined by matrix-assisted laser desorption/ionization mass spectrometry (MALDI) as well as by size exclusion chromatography (SEC). The number-average molecular weight of the P2VP-ah was determined to be 8 kg/mol from MALDI and 6 kg/mol from SEC.

Sample Preparation for DSIMS. A 300 nm thick SiO_2 layer was deposited on a Si wafer by plasma enhanced chemical vapor deposition (PECVD) to provide an insulating substrate for the DSIMS measurement. All samples were prepared by spin-casting a 350−400 nm thick layer of a mixture of P2VP homopolymer with a number-average molecular weight (M_n) of 152 kg/mol and P2VP-ah with M_n = 8 kg/mol from a solution in anhydrous pyridine. The volume ratio of P2VP-ah to P2VP homopolymers was kept as low as 0.01−0.02 for most experiments performed in this paper. The P2VP layer was then dried under vacuum for at least an hour to remove the residual solvent. A 450−500 nm thick layer of PS was then prepared on the top of the P2VP layer by spin-casting a mixture of 207 kg/mol PS homopolymer and dPS-NH_2 from toluene solution. Here, we used five different M_n of dPS-NH_2 ranging from 7 to 26 kg/mol while fixing M_n of P2VP-ah. The samples were annealed at various temperatures ranging from 130 to 180 °C in an ultrahigh vacuum oven at a pressure lower than 10^{-6} Torr in order to induce the reaction. After annealing, a float transfer method was used to prepare calibration layers for DSIMS in order to allow the deuterium signal from dPS-NH_2 to be related quantitatively to its volume fraction. A 150 nm thick PS film (M_n = 207 kg/mol) was floated on water from a glass slide and transferred on the top of the samples prepared above. Another 120 nm thick dPS film (M_n = 670 kg/mol) floated on water was subsequently transferred on top of the PS calibration layer by the same technique.

Dynamic Secondary Ion Mass Spectrometry (DSIMS). DSIMS is a well-established and widely used depth-profiling technique. Its strength includes relatively good depth resolution (∼8 nm) combined with high sensitivity and the ability to provide the profiles of all elements simultaneously. Particularly, DSIMS is very sensitive to deuterium. Therefore, DSIMS can be a useful tool to detect the diffusion and reaction of deuterium-labeled end-functionalized polymers. Our DSIMS experiments were performed using a Physical Electronics 6650 instrument in the MRL Central Facilities at UCSB. Negative ions are detected as polymer is sputtered by an incident beam of 3 keV O_2^+ ions. Our primary aim is to measure the interfacial excess of deuterium-labeled end-grafted PS at the PS/P2VP interface.

Results and Discussion

The excess amount of dPS-NH_2 at the interface between a PS layer and a P2VP layer during the reaction was monitored by analyzing the deuterium depth profile with DSIMS. This interfacial excess is the evidence of copolymer formation from the reaction of dPS-NH_2 chains with P2VP-ah chains, as shown in Figure 3. The dPS-NH_2 chains with M_n = 7 kg/mol and the P2VP-ah chains with M_n = 8 kg/mol in homopolymer layers were used for the reaction carried out for 10 h at 160 °C. The volume ratio of end-functionalized polymer to homopolymer in both PS and P2VP layers is 0.01. A typical DSIMS depth profile is shown in Figure 3. The interfacial excess z^* of dPS-NH_2 was determined by

$$z^* = \int^{\text{interface}} (\phi(z) - \phi_\infty)\, dz \qquad (1)$$

where $\phi(z)$ is the volume fraction of dPS-NH_2 at a depth z after annealing and ϕ_∞ is the volume fraction of dPS-NH_2 in the bulk of the PS film away from the interface. We denote a quantity $\xi_{PS} = z^*_{PS}/R_{g,PS}$ as this excess amount normalized by the radius of gyration of dPS-NH_2 ($R_{g,PS}$). A control experiment in which the P2VP layer contains no P2VP-ah chains resulted in zero interfacial excess of dPS-NH_2.

To study the reaction kinetics between dPS-NH_2 and P2VP-ah in our system, we measured $z^*_{PS}/R_{g,PS}$ (ξ_{PS}) values as a function of annealing time for each pair of dPS-NH_2 and P2VP-

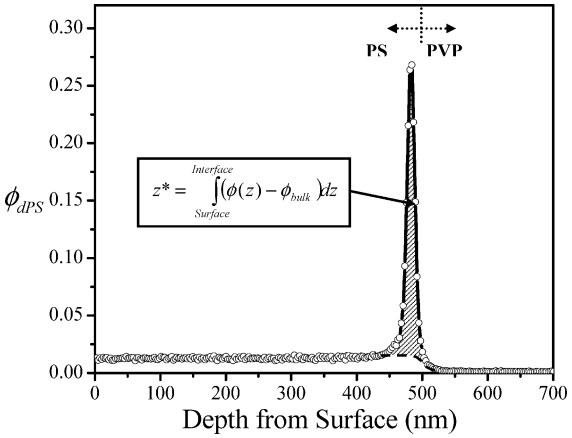

Figure 3. Volume fraction vs depth profile from DSIMS of dPS-NH_2 in a blend of dPS-NH_2 and PS at an interface with a blend of P2VP-ah and P2VP. The molecular weights of dPS-NH_2 and P2VP-ah are 7 and 8 kg/mol, respectively. A line with symbols represents dPS profile observed by DSIMS after 10 h annealing at 160 °C, and a dotted line represents unannealed dPS profile which has the same volume fraction of dPS-NH_2 in PS far from the interface. The interfacial integral excess z^* is represented by the shaded area.

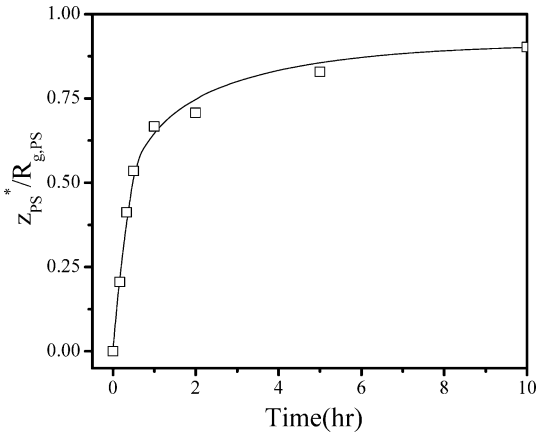

Figure 4. Normalized interfacial excess (ξ) as a function of annealing time at 160 °C for an initial volume fraction $\phi_0 = 0.01$. The molecular weights of dPS-NH_2 and P2VP-ah are 7 and 8 kg/mol, respectively.

ah at a fixed reaction temperature. Typical results for the normalized interfacial excess ξ_{PS} are shown in Figure 4 for dPS-NH_2 (M_n = 11 kg/mol) and P2VP-ah (M_n = 8 kg/mol) for various annealing times from 0 to 10 h at 160 °C. The initial volume fraction of end-functionalized polymer to homopolymer in both PS and P2VP layers is 0.01. Experimental points are shown as squares on the graph. Up to an annealing time of 5 h, there is a relatively rapid increase in ξ_{PS} followed by a decrease in rate, leading to saturation about $\xi_{PS} = 0.8$. These data can be analyzed by fitting them to the reaction kinetics model, which will be described in the following section.

A Reaction-Controlled Kinetics Model. As shown in Figure 1, dPS-P2VP diblock copolymers are formed at the interface by the reaction of dPS-NH_2 and P2VP-ah. Therefore, the model for reaction kinetics can be based on the second-order reaction as described in the following equation. The development of the model below follows a similar model developed by Jiao.[31]

$$\frac{d[\text{dPS-P2VP}]}{dt} = k^+[\text{dPS-NH}_2][\text{P2VP-ah}] - k^-[\text{dPS-P2VP}][\text{H}_2\text{O}] \quad (2)$$

where the brackets [ ] represent molecular concentrations. dPS-NH_2 will be denoted as A, P2VP-ah as B, and dPS-P2VP as C, for convenience. For generality, we have assumed that the reaction in Figure 1 goes all the way to the cyclic imide. If it does not (as we will argue below), [H_2O] can be eliminated from the subsequent equations, and $k^+$and k^- will refer to the reaction between the amine and the anhydride to form the amic acid.

Since diblock copolymers at the interface are formed from both the end-functionalized polymers, we can assume that the areal densities of the two end-functionalized polymers are equal

$$\Sigma_A = \frac{z^*_A}{N_A V_A} = \frac{\rho_0 \xi_A R_{g,A}}{N_A} = \frac{\rho_0 \xi_B R_{g,B}}{N_B} = \Sigma_B \quad (3)$$

In this equation, Σ_A and Σ_B are the areal densities of dPS-NH_2 and P2VP-ah, respectively, N_A and N_B are the degrees of polymerization of end-functionalized PS and PVP, respectively, V_A is the volume of dPS-NH_2, ξ_A and ξ_B are the normalized interfacial excess of dPS-NH_2 and P2VP-ah, respectively, and ρ_0 is the segmental density, which is assumed to be same for dPS-NH_2 and P2VP-ah.

Since diblock copolymers can be formed after two different end-functional polymers pay the entropy penalty for the localization of the chain end groups within a finite interfacial width δ, the free energy change of our system by reaction of end-functionalized polymers at the interface can be expressed after modification of Shull's result[26] as the following

$$\Delta G = \Delta G_{rxn} - 1.1RT \ln\left(\frac{\delta}{R_{g,A}}\right) - 1.1RT \ln\left(\frac{\delta}{R_{g,B}}\right) + \overline{\mu_c} N_{AV} \quad (4)$$

where ΔG_{rxn} is the free energy gain by the reaction of dPS-NH_2 and P2VP-ah end groups, δ is the interfacial width between PS and P2VP layers, N_{AV} is Avogardo's number, and $\overline{\mu_C}$ is the chemical potential arising from the entropy loss due to the stretching of the diblock copolymer blocks.

Therefore, the forward reaction rate coefficient (k^+) at chemical equilibrium can be expressed as the following

$$\frac{k^+}{k^-} = K_{rxn} = \exp\left(-\frac{\Delta G}{RT}\right) = \exp\left(-\frac{\Delta G_{rxn}}{RT}\right)\left(\frac{\delta}{R_{g,A}}\right)^{1.1}\left(\frac{\delta}{R_{g,B}}\right)^{1.1} \exp\left(-\frac{\overline{\mu_c}}{k_B T}\right) \quad (5)$$

where k^- represents the backward reaction rate coefficient and K_{rxn} is the equilibrium constant of the reaction.

Since the reaction occurs within a finite interfacial width δ, we can take the chain areal density of dPS-P2VP block copolymer to be $\Sigma_C = \Sigma_A = \delta$[C], where [C] is the molecular concentration of dPS-P2VP. Equation 2 becomes

$$\frac{d\Sigma_A}{dt} = k^+[A][B]\delta - k^-\Sigma_A[\text{H}_2\text{O}] \quad (6)$$

Since [A] = $\rho_0\phi_A/N_A$ and [B] = $\rho_0\phi_B/N_B$

$$\frac{d\xi_A}{dt} = \left(\left(\frac{\delta\phi_A\phi_B\rho_0}{R_{g,A}N_B}\right)k^+ - k^-\xi_A[\text{H}_2\text{O}]\right) \quad (7)$$

where ϕ_A and ϕ_B are the volume fractions of dPS-NH_2 and P2VP-ah in the PS and P2VP layers, respectively. Since we have finite reservoirs of dPS-NH_2 and P2VP-ah

$$z_A^* = (\phi_{A0} - \phi_A)h_A = \xi_A R_{g,A}$$

$$z_B^* = (\phi_{B0} - \phi_B)h_B = \xi_B R_{g,B} = \frac{N_B}{N_A}\xi_A R_{g,A} \quad (8)$$

where ϕ_{A0} and ϕ_{B0} are the initial volume fractions of dPS-NH_2 and P2VP-ah in the PS and P2VP layers, respectively, and h_A and h_B are the film thicknesses of the PS layer and P2VP layer, respectively.

Therefore, eq 7 can be expressed as the following:

$$\frac{d\xi_A}{dt} = \frac{\rho_0\phi_{A0}\phi_{B0}\delta}{N_B R_{gA}}k^+\left[1 - \frac{\xi_A R_{gA}}{h_A\phi_{A0}}\right]\left[1 - \frac{\xi_A R_{gA}}{h_B\phi_{B0}}\frac{N_B}{N_A}\right] - \frac{k^+}{K_{rxn}}\xi_A[H_2O]$$
$$= \lambda([1 - \alpha_1\xi_A][1 - \alpha_2\xi_A] - \beta\xi_A) \quad (9)$$

where

$$\lambda = \frac{\rho_0\phi_{A0}\phi_{B0}\delta}{N_B R_{gA}}k^+, \quad \alpha_1 = \frac{R_{gA}}{h_A\phi_{A0}}, \quad \alpha_2 = \frac{R_{gA}}{h_B\phi_{B0}}\frac{N_B}{N_A} \quad \text{and}$$
$$\beta = \frac{k^+[H_2O]}{K_{rxn}\lambda}$$

When chains are not stretched, such that $\overline{\mu_C}(\xi_A) = 0$ at a flat interface, this model predicts the forward reaction rate coefficient k^+ from eq 5

$$k^+ \sim (N_A N_B)^{-0.55}(\chi)^{-1.1} \sim {N_A}^{-0.55} \quad \text{(at fixed } N_B\text{)} \quad (10)$$

By fitting the data obtained by DSIMS results in Figure 4 to eq 9, values of λ and β were extracted. Then, they can be used to deduce the values of the forward reaction rate coefficient (k^+) and the backward reaction rate coefficient (k^-).

Study of the Effect of M_n of End-Functional Polymers on Reaction Kinetics. Five different dPS-NH_2 with molecular weights ranging from 7 to 26 kg/mol were used to study the effect of molecular weight on reaction kinetics. On the other hand, M_n of P2VP-ah is fixed at 8 kg/mol. As described in the Experimental Section, the initial volume fraction of each reactive polymer in its homopolymer matrix is set at 0.01−0.02 to prevent high copolymer areal chain densities that result in chain stretching as well as complex interfacial phenomena such as interfacial instability. The volume fraction of P2VP-ah in the P2VP matrix is kept as high or higher than that of dPS-NH_2 in PS matrix to make sure that the interfacial concentration of P2VP-ah would not be limiting factor for the reaction. Since the diffusion rate of the PS chains is the same or slower than the 8 kg/mol P2VP chains, the absence of a diffusion gradient of dPS near the interface on the PS side implies the absence of a diffusion gradient on the P2VP side.[14] Three different data series of the normalized interfacial excess (ξ_{PS}) of dPS-NH_2 with M_n = 7, 17, and 26 kg/mol are shown as a function of annealing time in Figure 5. The data were obtained at a reaction temperature of 130 °C. The data sets were fitted by the reaction controlled model as described in the previous section. The forward reaction rate coefficient (k^+) that was extracted from the fitting is shown in Figure 6 for five different dPS-NH_2 chains of different M_n. The actual concentration of reactive groups, obtained by correcting the volume fraction of the short chains (dPS-NH_2, P2VP-ah) for their functionality (Table 1), the fraction that have -NH_2 or -ah end groups on either side of the interface has been used in the fitting procedure. From the slope of this log−log scale plot, it can be seen that k^+ is proportional to M_n of the reactive dPS-NH_2 chains to the power of −0.70 ± 0.08. It should be noted that eq 10 predicts that $k^+ \sim N_{dPS}{}^{-0.55}$ at a bare interface, in rough agreement with the exponent found experimentally.

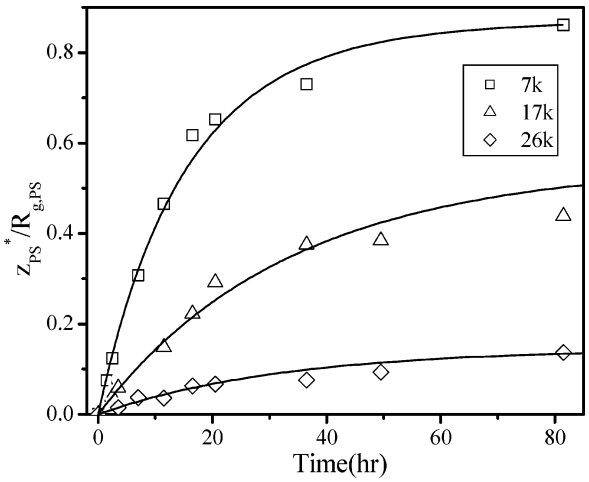

Figure 5. Normalized interfacial excess (ξ) as a function of annealing time for different molecular weights of dPS-NH_2. Squares, triangles, and diamonds represent ξ values for dPS-NH_2 with M_n = 7, 17, and 26 kg/mol, respectively. The lines represent the best fits to the reaction controlled model in the text.

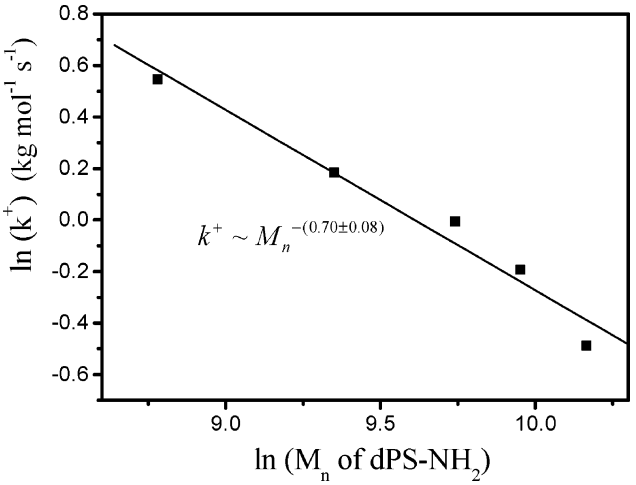

Figure 6. A log−log plot of the forward reaction rate coefficient (k^+) as a function of M_n of dPS-NH_2. From the slope of this plot, it was found that k^+ is proportional to M_n of reactive polymers with the power of −0.70 ± 0.08, which is in rough agreement with theoretical predictions ($k^+ \sim M_n{}^{-0.55}$).

Even though the two exponents, one from experiment and one from theoretical prediction, show similar values, it is worthwhile of pointing out possible factors that might cause the discrepancy between the two. One reason can be the assumption that the chain stretching penalty used in the reaction-controlled model can be neglected. We assume that all our experiments are performed in mushroom regime where block copolymers are not stretched significantly. According to theory, the parameter $\xi_{PS} = z^*_{PS}/R_{g,PS}$ provides the criteria how much polymer chains at the interface are stretched. Once ξ_{PS} becomes larger than 1, the area occupied by each polymer brush at the interface is smaller than the squared radius of gyration. Therefore, each individual polymer chain at the interface is affected by the interaction to others adjacent to it. Since all experiments in this paper were performed in the regime where ξ_{PS} is less than 1, the assumption used here is reasonable. In addition, since the P2VP-ah chains are shorter than dPS-NH_2 chains used in our experiment, the P2VP-ah chains at the

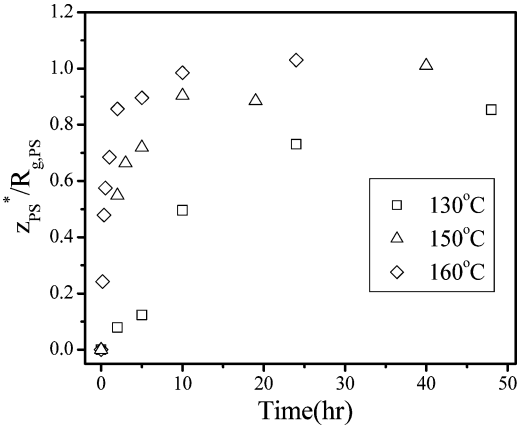

Figure 7. Normalized interfacial excess (ξ) as a function of annealing time for various reaction temperatures. Squares, triangles, and diamonds represent ξ values for samples of dPS-NH_2 (M_n = 7 kg/mol) and P2VP-ah (M_n = 8 kg/mol) annealed at 130, 150, and 160 °C, respectively.

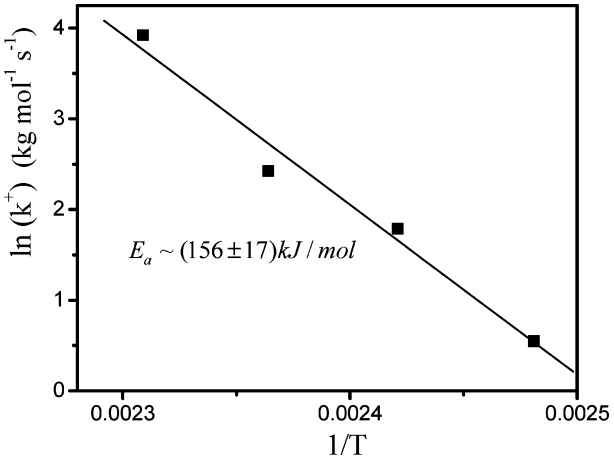

Figure 8. Forward reaction rate coefficient (k^+) is shown as a function of the inverse of reaction temperature for 7 kg/mol of dPS-NH_2 and P2VP-ah. From the slope of the graph, the activation energy is found to be 156 ± 17 kJ/mol.

interface in this experimental regime ($\xi_{PS} \ll 1$) are not expected to be stretched. However, when ξ_{PS} becomes closer to 1 in some parts of the experimental regime, especially at long annealing times, our approximation that the chain stretching penalty can be ignored (i.e., $\overline{\mu_C} = 0$) may underestimate the block copolymer chemical potential at the interface. Second, we want to point out that these experiments were carried out at low annealing temperatures so that the interfacial reaction is slow enough such that several different ξ_{PS} could be measured at annealing times that were not too short, allowing the growth of copolymer brush at the interface to be followed in detail. At short annealing times (<5−10 h), a slight gradient of dPS-NH_2 volume fraction is found next to the interface in the DSIMS depth profile, which indicates that the diffusion of the reactive polymer is not quite fast enough in this regime. This might influence the reaction kinetics in the early stages. The depth profile of the deuterium concentration becomes flat next to the interface after 10 h annealing, and all data after longer annealing times are unaffected. At higher temperature, diffusion is not a limiting factor at any reaction times, presumably because the diffusion coefficient of the short chains increases more rapidly with temperature than does k^+.[24]

Study of Reaction Temperature Effect on Reaction Kinetics. In the previous section, the effect of molecular weight of reactive polymers on reaction kinetics was studied. Here, dPS-NH_2 (M_n = 7 kg/mol) and P2VP-ah (M_n = 8 kg/mol) were used for examining the effect of various reaction temperatures. Four different reaction temperatures ranging from 130 to 160 °C were used. The initial volume fraction of reactive polymers in the homopolymer matrix was fixed at 0.01. The normalized interfacial excess ξ values of dPS-NH_2 at 130, 150, and 160 °C are plotted as a function of annealing time in Figure 7. As reaction temperature is increased, ξ_{PS} increases more rapidly with annealing time as expected, before eventually approaching an asymptotic value. Four different k^+ values at various reaction temperatures were extracted from these data sets and are plotted in Figure 8. As expected, the data are well described by an Arrhenius relation

$$k^+ = B \exp\left(-\frac{E_a}{k_B T}\right) \tag{11}$$

where E_a is the activation energy of reaction, k_B is Boltzmann's constant, T is reaction temperature, and B is T-independent. From the slope of Figure 8, the activation energy of reaction (E_a) is found to be 156 ± 17 kJ/mol. The value of the activation energy is not affected by the molecular weight of reactive polymers, since we also determined the activation energy, E_a, to be 164 kJ/mol for the different pair of dPS-NH_2 (M_n = 11 kg/mol) and P2VP-ah (M_n = 8 kg/mol). Jiao[27] found that the activation energy of the forward reaction between dPS-NH_2 and poly(styrene-*r*-maleic anhydride) (PSMA) is 207 kJ/mol, which is slightly higher than our value. He points out that this number might be overestimated due to the high viscosity of PSMA, since the reaction was performed between 170 and 190 °C, which is only slightly higher than the glass transition temperature of PSMA (163 °C). We also point out that the forward reaction rate coefficient (k^+) at 160 °C is only 30 times as high as that at 130 °C, while that the diffusion coefficient of relatively short PS and P2VP chains in the matrix of long PS and P2VP chains, respectively, increases by 3 orders of magnitude when the temperature is increased from 130 to 160 °C, as shown by Green and Kramer.[24] This fact reinforces our conclusion that the reaction kinetics in our system is not controlled by diffusion, but by the kinetics of the reaction at the interface.

Reversibility. In the previous section, we investigated the effect of molecular weight as well as reaction temperature on reaction kinetics. The result was explained well by our model built based on a reaction-controlled mechanism. In this section, we discuss the reversibility of the reaction. The scheme of this reaction is described in Figure 1. It is expected to be composed of two different steps. The first step is an initial ring-opening to form an amic acid group. This is expected to be followed by a condensation step to form a cyclic imide group under vacuum conditions. It is known that the ring-closing imidization step is much slower than the ring-opening amic acid-forming step.[23,28] It is expected that the second imidization step of our system should be an irreversible reaction, since the water activity in the vacuum oven must be extremely low. However, the result of fitting the reaction rate model to the observed kinetics showed consistently that our reaction is reversible, since the term β has a positive value, but small compared to k^+. To check the reversibility of the reaction, we designed an additional experiment as follows. One pair of reactive polymers of dPS-NH_2 (M_n = 11 kg/mol) and P2VP-ah (M_n = 8 kg/mol) was chosen. The volume fraction of reactive polymers in each homopolymer matrix was 0.01. First, three different pieces of the samples were prepared under identical conditions and annealed at 160 °C during enough time (i.e., 1 day) to produce an apparent

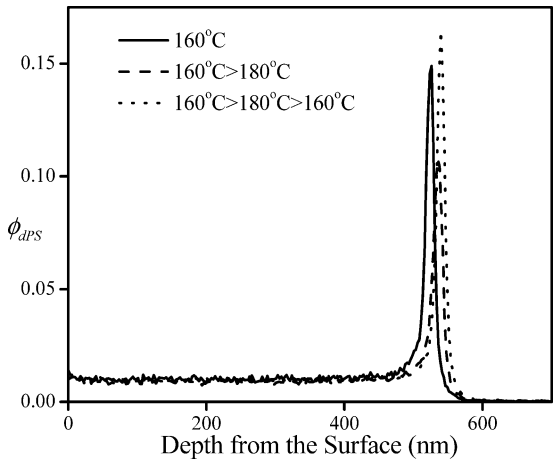

Figure 9. Volume fraction of dPS-NH_2 as a function of depth from the PS top surface obtained by DSIMS. Three different pieces of the samples A−C were prepared under identical conditions and annealed at 160 °C for enough time (i.e., 1 day) to achieve the equilibrium depth profile. Sample A (160 °C) was removed at this time. The 160 °C > 180 °C sample B was annealed at 180 °C for an additional 1 day. The 160 °C > 180 °C > 160 °C sample C was treated identically to B but then annealed further at 160 °C for 2 more days. The solid, dashed, and dotted lines represent samples A, B, and C, respectively.

equilibrium depth profile that does not change with further annealing. One of those pieces was taken out and quenched. The remaining two were annealed at 180 °C for one additional day. A second sample was quenched from this temperature. The remaining piece was annealed further at 160 °C for more 2 days to make sure that the depth profile is in equilibrium at that reaction temperature. All these samples were annealed continuously without being exposed to the air. For convenience, these three different samples are designated as samples A, B, and C, following the sequence in which they were taken out of the vacuum oven. The volume fractions vs depth profiles for the three samples are shown in Figure 9. The normalized interfacial excess (ξ_{PS}) of sample A annealed 1 day only at 160 °C is determined to be as 0.903 by DSIMS. The ξ_{PS} values of sample B and sample C were 0.716 and 0.971, respectively.

The difference in the amount of segregated diblock copolymers at different reaction temperatures might come from the temperature dependence of the equilibrium constant of the reaction, K_{rxn}. Since the ξ_{PS} value of sample C after three different annealing steps agrees reasonably well with that of sample A, it suggests that the reaction is reversible. The same kind of experiment was performed for the system where dPS-NH_2 (7 kg/mol) and P2VP-ah (8 kg/mol) were used. The results from this experiment agree well with those for dPS-NH_2 of (11 kg/mol) and P2VP-ah (8 kg/mol). We can rule out the possibility that some block copolymer formed at the interface at 160 °C desorbs from the interface and diffuses into either the PS or P2VP homopolymers based on the following two reasons. First, self-consistent-field theoretic simulations indicate that in equilibrium with the interfacial excess the volume fraction of dPS_{11K}-*b*-$P2VP_{8K}$ or dPS_{7K}-*b*-$P2VP_{8K}$ in either homopolymer layer should be negligible and could not account for the drop observed in going from 160 to 180 °C. Second, DSIMS can detect very small amounts of the dPS-*b*-P2VP in the P2VP homopolymer layer by measuring the $^2H^-$ signal from dPS or in the PS homopolymer layer by measuring the CN^- signal from P2VP. Under these reaction conditions the $^2H^-$ signal in the P2VP layer and the CN^- signal in the PS layer were at background levels. For clarification, the reversible and irreversible cases are illustrated in Scheme 1. In the reversible case, the $^2H^-$ signal

Scheme 1. As the Equilibrium Temperature Is Increased, the Amount of Diblock Copolymer Segregated at the Interface Is Reduced[a]

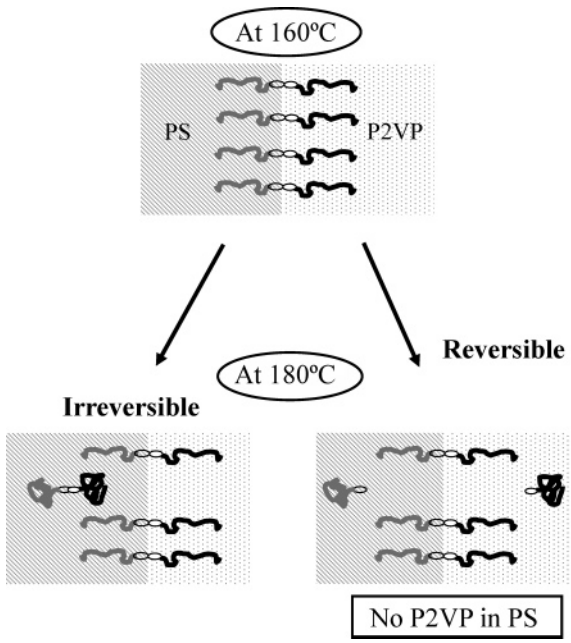

[a] Two different cases can be considered for the movement of the diblock copolymers. The left scheme on the bottom represents the case of irreversible reaction where diblock copolymers move into homopolymer layer without breaking into two different reactive polymers. The scheme on the right side represents the case of reversible reaction.

in the P2VP layer and the CN^- signal in the PS layer should be at background levels as confirmed by our experiment. Therefore, the decrease in ξ_{PS} on going from 160 to 180 °C must be due to the reversibility of the interfacial reaction.

Based on the reversibility of reaction, the equilibrium constant (K_{rxn}) can be calculated from $K_{rxn} = k^+/\beta\lambda$ in eq 9. Four different K_{rxn} values for 7 kg/mol of dPS-NH_2 and P2VP-ah with various temperatures ranging from 130 to 160 °C are calculated from the results of fitting data in Figure 7 as described for the procedure of k^+ calculation. As expected, the data are described by the relation

$$K_{rxn} = C \exp\left(-\frac{\Delta H_{rxn}}{k_B T}\right) \tag{12}$$

where ΔH_{rxn} is the standard enthalpy of reaction, k_B is Boltzmann's constant, T is reaction temperature, and C is a T-independent constant. To increase the reliability of the fitting by including more data, the equilibrium constants K_{rxn} for different temperatures are also estimated from the depth profile in equilibrium at the higher annealing temperature. As mentioned in Figure 9, three different samples with dPS_{11K}-$P2VP_{8K}$ or dPS_{7K}-$P2VP_{8K}$ end-functional chains were annealed to investigate the reaction reversibility. Since the all samples were annealed for a long time at high temperatures such as 160 and 180 °C, we assume that those samples are in equilibrium. Since $d\xi_A/dt = 0$ at equilibrium, eq 9 can be expressed as follows

$$K_{rxn} = \frac{\xi_A R_{gA} N_B}{\delta \rho_0 \phi_{A0} \phi_{B0}} \frac{1}{[1 - \alpha_1 \xi_A][1 - \alpha_2 \xi_A]} \tag{13}$$

where the interfacial width δ is estimated to be 1.6 nm for our PS−P2VP system.[29] At equilibrium, values of $\xi_A = 0.924$ at 160 °C and $\xi_A = 0.663$ at 180 °C for dPS_{7K}-*b*-$P2VP_{8K}$ were

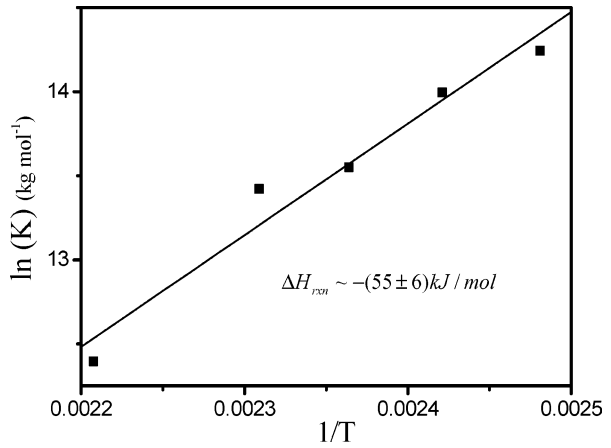

Figure 10. Equilibrium constant (K_{rxn}) is shown as a function of the inverse of reaction temperature for 7 kg/mol of dPS-NH_2 and P2VP-ah. From the slope of the graph, the extracted standard enthalpy of reaction (ΔH_{rxn}) is found to be $-(55 \pm 6)$ kJ/mol.

obtained, giving two different K_{rxn} values from eq 13. Five different K_{rxn} values obtained from the reaction temperatures ranging from 130 to 180 °C are plotted in Figure 10. (The value of K_{rxn} at 160 °C represents the average of the two different methods.) From the slope of Figure 10, the standard enthalpy of the reversible reaction (ΔH_{rxn}) is found to be $-(55 \pm 6)$ kJ/mol.

According to the reaction scheme shown in Figure 1, the kinetics of the intramolecular imidization should be of first order, but the actual kinetics are very complex and are affected by many physical and chemical factors.[30] Wang[31] showed that imidization of *N*-alkylmaleamic acids in acetic anhydride as both reagent and solvent and sodium acetate as a base yielded only very poor yields of the imides. In addition, he claimed that imidization favors aromatic amine substituents, whereas aliphatic primary amines react more rapidly with cyclic anhydrides to form the amic acid group due to stronger basicity. Furthermore, Grenire-Loustalot et al.[32] showed that the equilibrium between the amic acid group and the starting materials can dominate the subsequent dehydration reaction, leading to polyimide formation that depends on reaction conditions. Orr et al.[22] reported that the reaction coefficient for the first step of forming amic acid between amine end-functionalized PS and cyclic anhydride end-functionalized PS is 113 times as fast as that for imidization. Jiao[27] also found that the reaction between dPS-NH_2 and poly(styrene-*r*-maleic anhydride) (PSMA) is reversible. We think that in our system the equilibrium involving the amic acid of dPS-P2VP dominates the imidization step at the interface under our reaction conditions, perhaps because of the steric hindrance associated with the trimellitic anhydride. Therefore, the imidization step may be suppressed, becoming much slower than the reversible reaction of the first step. We cannot rule out however the possibility that suppression of imidization may be caused somehow by the presence of the interface. To do this would require an investigation of the homogeneous reaction between the same end groups on very short PS and P2VP polymers in a uniform melt, an investigation that is well beyond the scope of this paper.

Given the reversibility of the interface reaction, it is of interest to estimate the maximum change in interfacial tension[14] at an initial end-functional polymer volume fraction of 0.01 (keeping $(\phi_{dPS-NH_2})_0 = (\phi_{P2VP-ah})_0$ as well as the value of the initial and equal volume fractions necessary to reduce the interfacial tension to near zero). Table 2 shows the predicted results for bilayer films of PS and P2VP with thicknesses of 500 nm each at equilibrium at 180 °C. The results show that the interfacial tension at 0.01 initial volume fraction of dPS-NH_2 and P2VP-ah is always positive at this temperature and increases with M_n of dPS-NH_2. Correspondingly, as M_n of dPS-NH_2 increases, the initial volume fraction required to achieve near zero interfacial tension under final equilibrium conditions increases. The comparison of these predictions with the experimentally measured onset of interfacial roughening will be the subject of a separate paper in preparation.

Table 2. Predicted Decrease in Interfacial Tension for End-Functional Polymers of Molecular Weight M_n

M_n (kg/mol)	$z^*_{PS}/R_{g,PS}$ in equilibrium at 180 °C	$(\Delta\gamma/\gamma_0)_{max}$[a]	$(\phi_0)_{dPS}$[b]
7	0.656	−0.47	0.016
11	0.579	−0.34	0.019
17	0.498	−0.25	0.023
21	0.457	−0.19	0.025
26	0.418	−0.15	0.028

[a] Estimated decrease in interfacial tension in equilibrium at 180 °C for initial volume fractions of dPS-NH_2 and P2VP-ah of 0.01. [b] Estimated initial volume fractions of dPS-NH_2 and P2VP-ah required to achieve zero interfacial tension at 180 °C, assuming all chains have 100% end-functionality.

Conclusions

In this paper, the reaction kinetics of dPS-NH_2 and P2VP-ah at the melt interface between PS and P2VP has been investigated experimentally. The interfacial excess (z^*) of block copolymer formed by the reaction of dPS-NH_2 and P2VP-ah at the interface was quantified by DSIMS measurement for different reaction times as a function of molecular weight (M_n) of the end-functional polymers and reaction temperatures. The reaction kinetics is analyzed by a model based on a reaction controlled mechanism in the low grafting regime, such that the normalized interface excess (z^*/R_g) < 1 and the blocks are unstretched. In this regime, the forward reaction rate constant (k^+) decreases as $M_n^{-0.70}$, in rough agreement with theoretical predictions ($k^+ \sim M_n^{-0.55}$). The reaction is thermally activated with an activation enthalpy (~160 kJ/mol) that is independent of M_n. Surprisingly, the interfacial reaction to form the diblock copolymer turns out to be reversible, which implies that the reaction stops at the amic acid rather than proceeding irreversibly to the imide.

Acknowledgment. We acknowledge the support of the UCSB Materials Research Lab. (NSF-DMR-MRSEC Grant DMR05-20415). The skillful help of Dr. Tom Mates with DSIMS and Dr. Krystyna Brzezinska with synthesis is greatly appreciated. We also acknowledge Dr. Huiman Kang and Prof. Kookheon Char, whose contributions to the early stage of this research were particularly helpful.

References and Notes

(1) Leibler, L. *Makromol. Chem., Macromol. Symp.* **1988**, *16*, 1−17.
(2) Shull, K. R.; Winey, K. I.; Thomas, E. L.; Kramer, E. J. *Macromolecules* **1991**, *24*, 2748−2751.
(3) Fredrickson, G. H. *Phys. Rev. Lett.* **1996**, *76*, 3440−3443.
(4) Fredrickson, G. H.; Milner, S. T. *Macromolecules* **1996**, *29*, 7386−7390.
(5) Kramer, E. J. *Isr. J. Chem.* **1995**, *35*, 49−54.
(6) O'Shaughnessy, B.; Sawhney, U. *Macromolecules* **1996**, *29*, 7230−7239.
(7) O'Shaughnessy, B.; Sawhney, U. *Phys. Rev. Lett.* **1996**, *76*, 3444−3447.
(8) Muller, M. *Macromolecules* **1997**, *30*, 6353−6357.
(9) Oyama, H. T.; Inoue, T. *Macromolecules* **2001**, *34*, 3331−3338.
(10) Yin, Z.; Koulic, C.; Pagnoulle, C.; Jerome, R. *Macromol. Symp.* **2003**, *198*, 197−208.

(11) Yin, Z.; Koulic, C.; Pagnoulle, C.; Jerome, R. *Can. J. Chem. Eng.* **2002**, *80*, 1044−1050.
(12) Yin, Z.; Koulic, C.; Pagnoulle, C.; Jerome, R. *Macromolecules* **2001**, *34*, 5132−5139.
(13) Jeon, H. K.; Kim, J. K. *Macromolecules* **2000**, *33*, 8200−8210.
(14) Kim, B. J.; Kang, H.; Char, K.; Katsov, K.; Fredrickson, G. H.; Kramer, E. J. *Macromolecules* **2005**, *38*, 6106−6114.
(15) Kim, H. Y.; Jeong, U.; Kim, J. K. *Macromolecules* **2003**, *36*, 1594−1602.
(16) Schulze, J. S.; Cernohous, J. J.; Hirao, A.; Lodge, T. P.; Macosko, C. W. *Macromolecules* **2000**, *33*, 1191−1198.
(17) Schulze, J. S.; Moon, B.; Lodge, T. P.; Macosko, C. W. *Macromolecules* **2001**, *34*, 200−205.
(18) Yin, Z.; Koulic, C.; Pagnoulle, C.; Jerome, R. *Langmuir* **2003**, *19*, 453−457.
(19) Jones, T. D.; Schulze, J. S.; Macosko, C. W.; Lodge, T. P. *Macromolecules* **2003**, *36*, 7212−7219.
(20) Lyu, S. P.; Cernohous, J. J.; Bates, F. S.; Macosko, C. W. *Macromolecules* **1999**, *32*, 106−110.
(21) Zhang, J. B.; Lodge, T. P.; Macosko, C. W. *Macromolecules* **2005**, *38*, 6586−6591.
(22) Orr, C. A.; Cernohous, J. J.; Guegan, P.; Hirao, A.; Jeon, H. K.; Macosko, C. W. *Polymer* **2001**, *42*, 8171−8178.
(23) Padwa, A. R.; Sasaki, Y.; Wolske, K. A.; Macosko, C. W. *J. Polym. Sci., Part A: Polym. Chem.* **1995**, *33*, 2165−2174.
(24) Green, P. F.; Kramer, E. J. *J. Mater. Res.* **1986**, *1*, 202−4.
(25) Weis, C.; Friedrich, C.; Mulhaupt, R.; Frey, H. *Macromolecules* **1995**, *28*, 403−405.
(26) Shull, K. R. *J. Chem. Phys.* **1991**, *94*, 5723−5738.
(27) Jiao, J. B. Ph.D. Thesis, Cornell University, 1997.
(28) Scott, C.; Macosko, C. *J. Polym. Sci., Part B: Polym. Phys.* **1994**, *32*, 205−213.
(29) Dai, K. H.; Norton, L. J.; Kramer, E. J. *Macromolecules* **1994**, *27*, 1949−1956.
(30) Kim, Y. J.; Glass, T. E.; Lyle, G. D.; Mcgrath, J. E. *Macromolecules* **1993**, *26*, 1344−1358.
(31) Wang, Z. Y. *Synth. Commun.* **1990**, *20*, 1607−1610.
(32) Grenier-Loustalot, M. F.; Joubert, F.; Grenier, P. *J. Polym. Sci., Part A: Polym. Chem.* **1991**, *29*, 1649−1660.
(33) Macosko, C. W.; Jeon, H. K.; Hoye, T. R. *Prog. Polym. Sci.* **2005**, *30*, 939−947.
(34) Zhang, J.; Lodge, T. P.; Macosko, C. W. *Bull. Am. Phys. Soc.* **2006**, *51*, 639−639.
(35) Harton, S. E.; Stevie, F. A.; Ade, H. *Macromolecules* **2005**, *38*, 3543−3546.

MA0611218